International Journal of Technical Innovation in Modern Engineering & Science (IJTIMES)
Impact Factor: 3.45 (SJIF-2015), e-ISSN: 2455-2585
Volume 4, Issue 01, January-2018

NUMERICAL MODELLING FOR STUDIES ON SUPERSONIC FLOW OVER A CAVITY WITH SPOILER INVOLVING VELOCITY FIELD AND OVERALL SOUND PRESSURE LEVEL BY LES-APPROACH

Dr. Nirmal Kumar Kund

Associate Professor, Department of Production Engineering
Veer Surendra Sai University of Technology, Burla 768018, India

Abstract*— The present investigation pertains to the development of an appropriate numerical model for the supersonic flow over a 3D cavity with a length-to-depth ratio of 2. The Mach number of the supersonic free-stream is 2 in addition the Reynolds number of the flow is 10^5. The numerical simulations have been conducted by means of Large Eddy Simulation (LES) method. The Smagorinky model is introduced for this research. The numerical predictions have been expressed in the form of velocity vector as well as overall sound pressure level along the side wall of the open cavity. As witnessed, the velocity vector superbly describes the flow behaviour inside the cavity. Very large recirculation is also noticed inside the cavity without spoiler. Nevertheless, the reduction of the recirculation inside the cavity is realized by introducing a spoiler in the form of one-fourth of a cylinder at the leading edge of the open cavity. With the introduction of the spoiler, the overall sound pressure level along the side wall of the cavity is also decreased to certain level. Correspondingly, the sound pressure levels get decreased by almost 14 dB and 12 dB at both front and aft walls of the cavity, respectively. The alterations in the flow characteristics of the cavity along with the spoiler is also examined. In general, the comparisons between the simulation predictions of the cavity flows with and without the use of the spoiler is also made.

***Keywords*— Numerical Simulation, Open Cavity, Spoiler, LES, Velocity Vector, OASPL.**

I. INTRODUCTION

The aerodynamic forces experienced by the surface of the moving bodies cause enormous noise which is a very supreme and dynamic challenge in numerous automotive and engineering habits. Airframe noise is a major part of overall noise, primarily during landing and take-off. Noise from landing gear, flaps, slats etc. are called as airframe noise. One of the greatest vital airframe noises is the cavity noise. It is generated from open wheel wells after the undercarriage while landing. The weapon bays in the military aircrafts involve oscillations induced by the flow, which can stimulate the vibrational modes of the structure of the aircraft. At low Mach numbers for surface transport, the automotive sectors are worried with the noises caused from the door gaps, side mirrors, and the open sun roof. These noises groups also affect the comfort in the conveyances.

The door gaps, wheel wells as well as weapon bays are modelled as rectangular cavities and the serene flow outside the cavity is taken to be smooth. Although the rectangular cavity is simple in shape, it is rich in different dynamic and acoustic phenomena, likely covered by an aeroacoustic feedback loop depending on the shape/size of the cavity as well as the flow situations. Very large intensity noises are produced on account of the vortex shredding at the upstream edge of the cavity, during the flow past a cavity.

The flow-induced pressure oscillations in shallow cavities are described by Heller et al. [1]. The investigations on the tones and pressure oscillations induced by flow over rectangular cavities are carried out by Tam and Block [2]. Mach 0.6 to 3.0 flows over rectangular cavities are performed by Kaufman et al. [3]. The high resolution schemes are used by Sweby [4] in applying flux limiters on hyperbolic conservation laws. The numerical simulation on supersonic flow over a 3D cavity are reported by Rizzetta [5]. The very fundamentals of computational fluid dynamics is demonstrated by Anderson and Wendt [6]. The achievements and challenges of large-eddy simulation are described by Piomelli [7]. The numerical simulations of fluidic control for transonic cavity flows are carried out by Hamed et al. [8]. The LES studies on feedback-loop mechanism of supersonic open cavity flows are conducted by Li et al. [9]. A validation study on unsteady RANS computations of supersonic flow over 2D cavity is done by Vijayakrishnan [10]. The lid-driven cavity flows of viscoelastic liquids are very well illustrated by Sousa et al. [11]. The experimental investigations on double-cavity flows are studied by Tuerke et al. [12]. It is perceived that a broad study on cavity flow has been done both experimentally and computationally for enhancing the aerodynamic effectiveness. However, apart from its prominence, the complicated flow physics of flow past a cavity has mesmerised the investigators around the world for further researches and it still remains to be a thrust field of research.

Even if, quite a large number of experiments have been conducted to reduce the recirculation inside the cavity, yet, some are not just effective for complete flow situations. The performance of the control devices are ominously influenced by the Mach number. Control devices must be designed so that they work over a wide range of Mach numbers. The incoming boundary layer is also another vital factor which influences the performance of the control devices. Keeping this perspective in attention, the drive of this investigation is to study the flow phenomenon in a three-dimensional open cavity supersonic flow. Also, the reduction of recirculation inside the cavity by passive method has been investigated by introducing a spoiler at the leading edge of the cavity. The comparison between the open cavity flows with and without the use of spoiler has also been made. In general, the present researches pertain to the development of a 3D numerical model for comparative simulation predictions of the open cavity flows expressed in terms of velocity vector and overall sound pressure level (OASPL) along the side wall of the open cavity with and without the introduction of the spoilers.

II. DESCRIPTION OF PHYSICAL PROBLEM

Supersonic flow past a three-dimensional cavity is studied numerically. The streamwise length, depth and spanwise length of the cavity are 20 mm, 10 mm, and 10 mm, respectively. The length-to-depth ratio (L/D) for the cavity is 2. The width-to-depth ratio (W/D) is 1. The cavity is three-dimensional with streamwise length-to-spanwise length ratio (L/W) > 1. In addition, the Mach number of the free-stream along with the Reynolds number based on the cavity depth are taken as 2 and 10^5, respectively, for setting the inflow conditions.

2.1. Geometric Model

The computational domain of the cavity with the spoiler is shown in figure 1. The size of this domain, as stated previously, is 2D×D×D (length × depth × width). The spoiler at the cavity leading edge has a dimension of 0.6D. One-fourth part of a cylinder has been used for the shape of the spoiler. The domain is three-dimensional with $L/W > 1$. The upper boundary is at a distance of 4D above the cavity to ensure that no reflected shock affects the flow features inside the cavity.

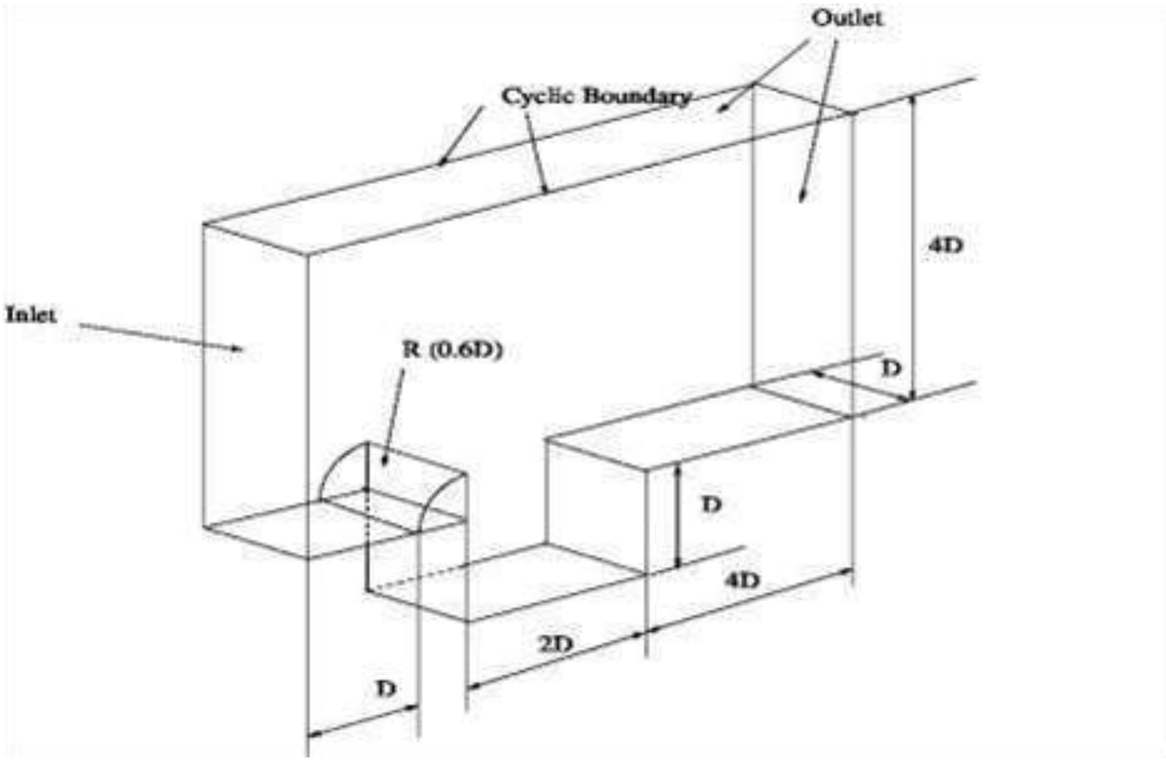

Fig 1. Computational domain of cavity with spoiler

2.2. Initial and Boundary Conditions

The initial conditions for the cavity involving supersonic flow are Mach number = 2 with P_∞ = 101.325 kPa and T_∞ = 300 K at the inlet, Reynolds number of the flow being 10^5, based on the cavity depth.

No-slip adiabatic wall boundary conditions is applied at the wall boundaries. Zero-gradient condition is applied at all the outflow boundaries. Periodical boundary condition is applied in the spanwise direction of the cavity. No-slip adiabatic wall boundary condition is employed for the spoiler.

III. MATHEMATICAL FORMULATION

3.1. Generalized Governing Transport Equations

The 3D compressible Navier-Stokes equations are the governing equations which comprise the continuity equation (1), the momentum equation (2), and the energy equation (3) which are as mentioned below:

$$\frac{\partial \rho}{\partial t} + \nabla.(\rho \boldsymbol{U}) = 0 \qquad (1)$$

$$\frac{\partial(\rho \boldsymbol{U})}{\partial t} + \nabla.(\rho \boldsymbol{U}.\boldsymbol{U}) - \nabla.\nabla(\mu \boldsymbol{U}) = -\nabla p \qquad (2)$$

$$\frac{\partial(\rho e)}{\partial t} + \nabla.(\rho e \boldsymbol{U}) - \nabla.\nabla(\mu e) = -p(\nabla.\boldsymbol{U}) + \mu\left[\frac{1}{2}(\nabla \boldsymbol{U} + \nabla \boldsymbol{U}^{\mathrm{T}})\right]^2 \qquad (3)$$

Where, $\boldsymbol{U}$ = velocity vector = $u\hat{\imath} + v\hat{\jmath} + w\hat{k}$ and $\frac{1}{2}(\nabla \boldsymbol{U} + \nabla \boldsymbol{U}^{\mathrm{T}})$ = strain rate tensor.

The equations (1), (2) and (3) symbolise the conservation form of the Navier-Stokes equations. The conservation form of these governing equations are reached from a flow model fixed in space [6]. The stated equations are relevant to viscous flow, except that the mass diffusion is not involved.
It is supposed, in aerodynamics, that the gas is a perfect gas. The equation of state for a perfect gas is, $p = \rho RT$ (4)

Where, R = specific gas constant = C_p - C_v (5)

For a calorically perfect gas (constant specific heats), the caloric equation of state is,
e = internal energy per unit mass = C_vT (6)

3.2. LES Turbulence Modelling

The turbulent flows may be simulated applying three different methods: Reynolds-Averaged Navier-Stokes equations (RANS), direct numerical simulation (DNS), and large eddy simulation (LES). Direct numerical simulation has high computational necessities. DNS resolves all the scales of motion and for this it desires a number of grid points proportional to $(Re)^{9/4}$ and computational scales' cost is proportional to $(Re)^3$ [7].

In the current investigation, behaviours of the turbulent flow field have been simulated applying LES as it is suitable for unsteady complex flows and noise induced flows. LES computes the large resolved scales and also models the smallest scales. The turbulence model is incorporated by dividing the time and space varying flow parameters into two components, the resolved one $\bar{f}$ and f', the unresolved portion:

$$(x,t) = \bar{f}(x,t) + f'(x,t) \qquad (7)$$

LES usages a filtering operation to separate these resolved scales from the unresolved scales. The filtered parameter is represented by an over bar [7]. The top-hat filter smooth both the fluctuations of the large-scale as well as those of small scales. The filtering operation whenever introduced to the Navier-Stokes equation, it results in:

$$\frac{\partial \bar{\rho}}{\partial t} + \nabla.(\overline{\rho \boldsymbol{U}}) = 0 \qquad (8)$$

$$\frac{\partial(\overline{\rho \boldsymbol{U}})}{\partial t} + \nabla.(\overline{\rho \boldsymbol{U}.\boldsymbol{U}}) - \nabla.\nabla(\overline{\mu \boldsymbol{U}}) = -\nabla \bar{p} \qquad (9)$$

$$\frac{\partial(\overline{\rho e})}{\partial t} + \nabla.(\overline{\rho \boldsymbol{U} e}) - \nabla.\nabla(\overline{\mu e}) = -\overline{p(\nabla.\boldsymbol{U})} + \mu\left[\frac{1}{2}(\nabla \bar{\boldsymbol{U}} + \nabla \bar{\boldsymbol{U}}^{\mathrm{T}})\right]^2 \qquad (10)$$

Nevertheless, the dissipative scales of motion are rectified poorly by LES. In a turbulent flow, the energy from the large resolved structures are passed on to the smaller unresolved structures by an inertial and an effective inviscid mechanism. This is called as energy cascade. Therefore, LES employs a sub-grid scale model to mimic the drain pertaining to this energy cascade. Most of these models are eddy viscosity models connecting the subgrid-scale stresses (τ_{ij}) and the resolved-scale rate of strain-tensor ($\bar{S}_{ij}$),

$$\tau_{ij} - (\delta_{ij}/3) = -2\nu_T \bar{S}_{ij} \quad (11)$$

Where, $\bar{S}_{ij}$ is the resolved-scale rate of strain tensor = $(\partial \bar{u}_i/\partial x_j + \partial \bar{u}_j/\partial x_i)/2$.
In most of the circumstances it is supposed that all the energy received by the unresolved-scales are dissipated instantly. This is the equilibrium assumption, i.e., the small-scales are in equilibrium [7]. This simplifies the problem to a great extent and an algebraic model is found for the eddy viscosity:

$$\mu_{sgs} = \rho C \Delta^2 |\bar{S}| \bar{S}_{ij},\ |\bar{S}| = (2\bar{S}_{ij}\bar{S}_{ij})^{1/2} \quad (12)$$

Here, Δ is the grid size and is generally considered to be the cube root of the cell volume [7]. This model is termed as the Smagorinsky model and C is the Smagorinsky coefficient. In the current investigation, its value has been considered to be 0.2.

IV. NUMERICAL PROCEDURES

4.1. Numerical Scheme and Solution Algorithm

The 3D compressible Navier-Stokes governing transport equations are discretized over an outline concerning finite volume method (FVM) through the SIMPLER algorithm. Here, the turbulent model utilized for large eddy simulation is Smagorinsky model, on account of its minimalism. The spatial derivatives like Laplacian and convective terms are computed by second order scheme based on Gauss theorem. Furthermore, the viscous terms are calculated by second order scheme. Additionally, the implicit second order scheme is utilized for time integration. The numerical fluxes are calculated by using Sweby limiter in central differencing (CD) scheme, which is a total variation diminishing (TVD) scheme. The central differencing (CD) is an unbounded second order scheme, while, the total variation diminishing (TVD) is a limited linear scheme. The developed solver is utilized to predict flow behaviours of the related flow variables pertaining to supersonic flow over an open cavity.

4.2. Choice of Grid Size, Time Step and Convergence Criteria

The computational domain is again decomposed into upper cavity and inside cavity region as illustrated in figure 2. The grid is refined at the regions near to the wall (where very high gradient is expected) to determine the behaviour of shear layer satisfactorily. A comprehensive grid-independence test is performed to establish a suitable spatial discretization, and the levels of iteration convergence criteria to be used. As an outcome of this test, the optimum number of grid points used for the final simulation, in the upper cavity region as 360 × 150 × 1 and those of in the inside cavity region as 200 × 150 × 1. The grid spacing at the leading edge of the cavity denoted as ΔX^+, ΔY^+ and ΔZ^+ being 5.0, 12.5, and 1.0, respectively. However, the total number of grid points is 81000 for this cavity. Corresponding time step chosen in the numerical simulation is 10^{-6} seconds. Even though, it is tested with smaller grids of 128000 in numbers, it is witnessed that a finer grid structure does not change the results considerably.

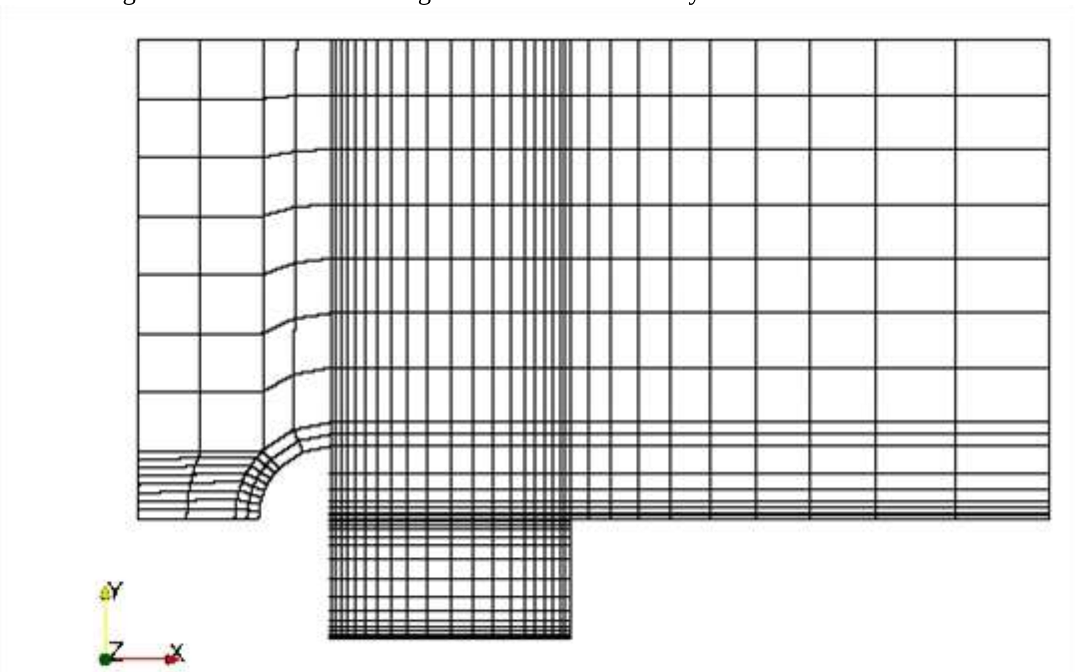

Fig 2. Computational grid of cavity with spoiler in X-Y Plane

The convergence in inner iterations is confirmed only when the condition $\left|\frac{\varphi - \varphi_{old}}{\varphi_{max}}\right| \le 10^{-4}$ is fulfilled concurrently for all variables, where φ represents the field variable at a grid point at the current iteration level, φ_{old} stands for the corresponding value at the previous iteration level, and φ_{max} is the maximum value of the variable at the current iteration level in the whole domain.

V. RESULTS AND DISCUSSIONS

The recirculation must be suppressed inside the open cavity. Furthermore, the noise created because of the flow past the stated cavity require to be diminished. This may be realized by introducing a spoiler at the leading edge of the cavity. The spoiler used in the current investigation is one-fourth part of a cylinder.

5.1. Comparisons of Velocity Distributions with and without Spoiler

The velocity vectors, at an instant of time t = 0.2 sec, for supersonic flow over an open cavity with and without the practice of spoiler are demonstrated in the figure 3. The velocity vector shows the recirculation inside the cavity. The flow behaviour over the cavity with spoiler is different from that of the cavity without spoiler which can simply be noticed from the velocity vectors. One shedding vortex is realized in the cavity with spoiler contrary to two shedding vortices witnessed in the cavity without spoiler. The recirculation zones of both the cavities are very different from one another. The velocity vectors pertaining to supersonic flow over the open cavity with and without the use of spoiler, at one more instant of time t = 0.4 sec, are also illustrated in the figure 4. The variations in the flow characteristics may also be understood from both the said figures presented at two different instants of times.

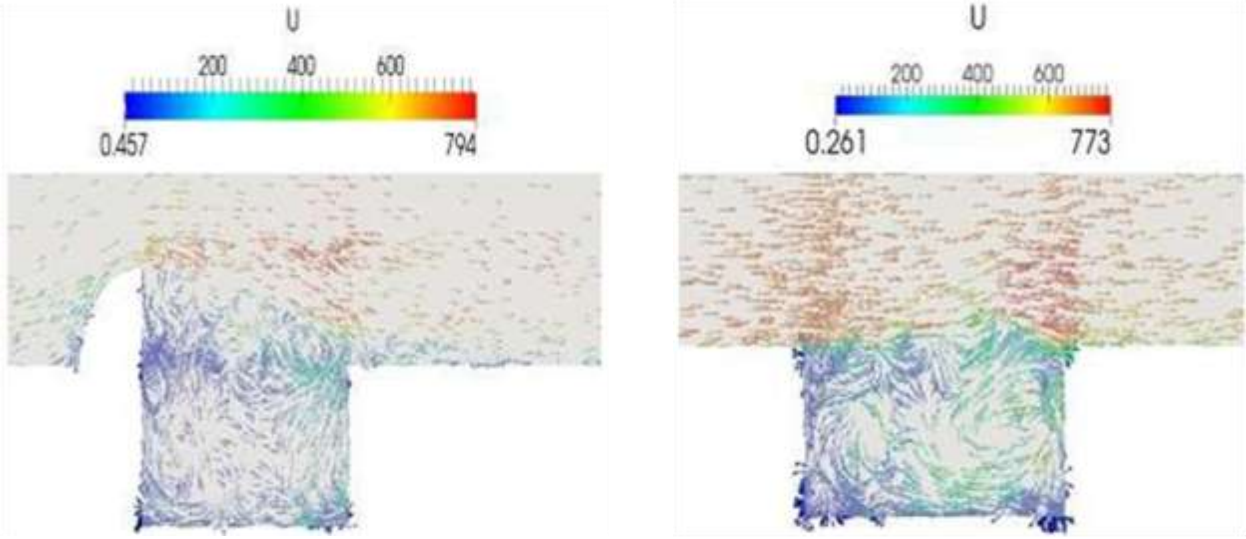

(a) With Spoiler (b) Without Spoiler

Fig 3. Velocity vector at instant of time, t = 0.2 sec, with and without the use of spoiler

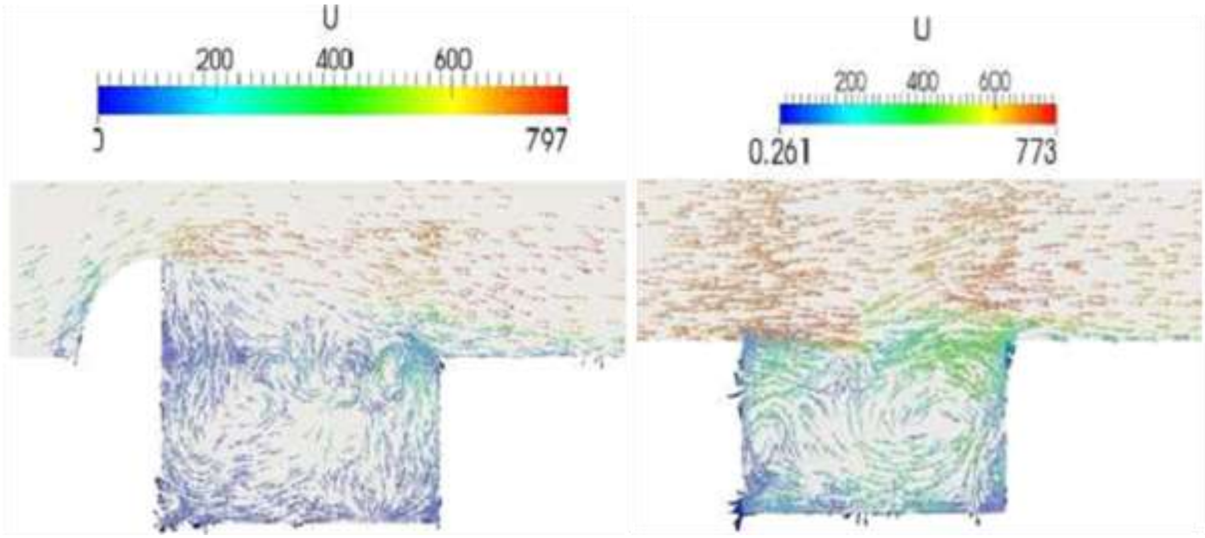

(a) With Spoiler (b) Without Spoiler

Fig 4. Velocity vector at instant of time, t = 0.4 sec, with and without the use of spoiler

5.2. Comparisons of Overall Sound Pressure Level (OASPL) with and without Spoiler

The comparison of the OASPL (Overall Sound Pressure Level) distributions along the side wall of the open cavity with and without the use of spoiler has also been made. The OASPL is denoted as:

$$OASPL = 10\, log_{10}\left(\overline{p_d^2}/q^2\right) \tag{13}$$

Where, $$\overline{p_d^2} = \frac{1}{t_f - t_i}\int_{t_i}^{t_f} (p - \bar{p})^2\, dt \tag{14}$$

q is the acoustic sound reference level with a value equal to 2×10^{-5} Pa

$\bar{p}$ is the time-averaged static pressure

t_f and t_i are the initial and final times, respectively

The OASPL distribution along the side wall of the cavity with spoiler has been compared with that of without the usage of spoiler. The comparison of both the above-mentioned circumstances are presented in the figure 5. It is noticed that on an average the OASPL gets decreased by around 10 dB. However, it is further noticed that the OASPL is decreased by almost 12 dB at the aft wall of the cavity and also gets decreased by almost 14 dB at the front wall of the cavity.

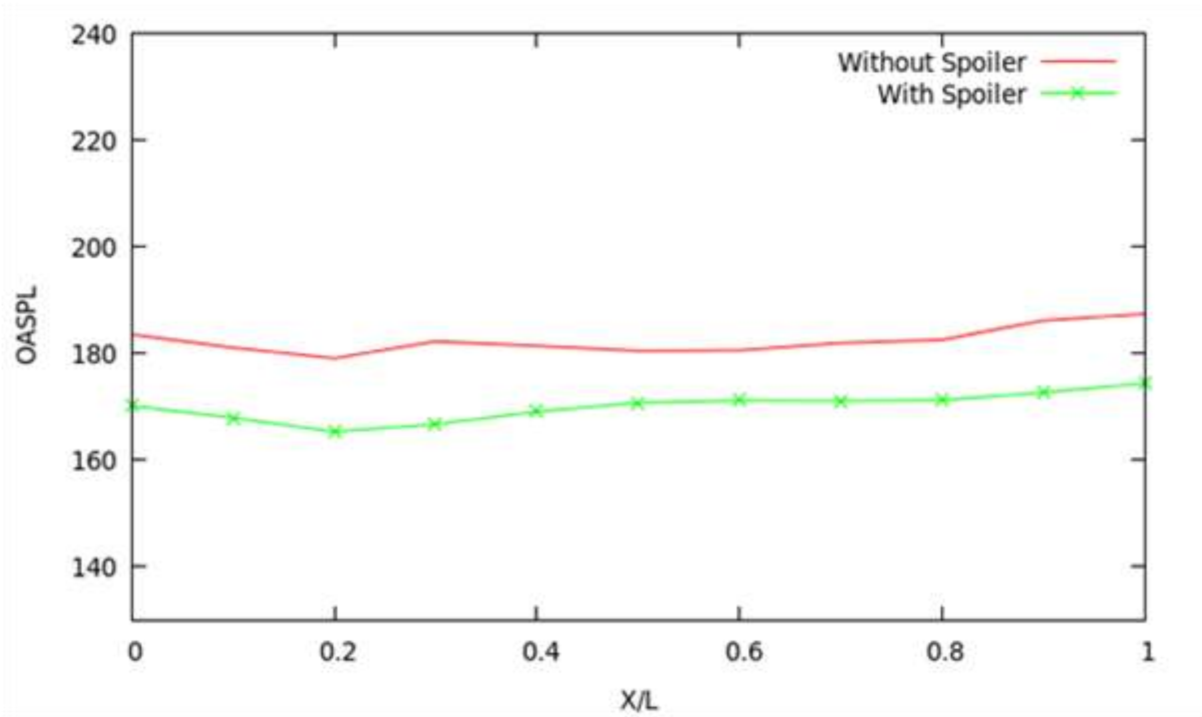

Fig 5. OASPL distribution along the side wall of the cavity with and without the use of spoiler

VI. CONCLUSIONS

In the current effort, the numerical simulation has been conducted for supersonic flow over an open cavity with and without the introduction of spoiler. The cavity has length-to-depth ratio of 2 in addition Mach number of the free-stream is 2.0. The simulation is performed by considering LES based Smagorinsky model. The simulation predictions are expressed in the form of both cavity flow-field analysis represented by velocity vectors as well as the aeroacoustic analysis expressed as the overall sound pressure level along the side wall of the cavity. The LES model is capable of predicting all the key flow characteristics of the cavity. The overall sound pressure level along the side wall of the cavity with spoiler is compared with that of without the spoiler. There exists both qualitative and quantitative agreement between the two, as the trends of results for both the cavities are very similar and therefore are comparable. Nevertheless, with the introduction of spoiler the average sound pressure level along the side wall of the cavity gets reduced by about 10 dB, whereas, the sound pressure levels also get decreased by almost 12 dB and 14 dB at both aft and front walls of the cavity, respectively. In general, in the current investigation, a 3D model is established for supersonic flow over a cavity and a spoiler is introduced at its leading edge to examine the flow characteristics and to reduce the recirculation inside the cavity. Furthermore, the overall sound pressure level along the side wall of the cavity is also witnessed to be reduced.

Acknowledgments

The author would like to thank the editor and the reviewers for extending their constructive views, valuable time and contributions for giving perceptive reviews to the research article.

REFERENCES

[1] Heller, H. H., Holmes, D. G., & Covert, E. E. (1971). Flow-induced pressure oscillations in shallow cavities. Journal of sound and Vibration, 18(4), 545-553.

[2] Tam, C. K., & Block, P. J. (1978). On the tones and pressure oscillations induced by flow over rectangular cavities. Journal of Fluid Mechanics, 89(02), 373-399.

[3] Kaufman, I. I., Louis, G., Maciulaitis, A., & Clark, R. L. (1983). Mach 0.6 to 3.0 flows over rectangular cavities (No. AFWAL-TR-82-3112). Air force wright aeronautical labs wright-patterson AFB, OH.

[4] Sweby, P. K. (1984). High resolution schemes using flux limiters for hyperbolic conservation laws. SIAM journal on numerical analysis, 21(5), 995-1011.

[5] Rizzetta, D. P. (1988). Numerical simulation of supersonic flow over a three-dimensional cavity. AIAA journal, 26(7), 799-807.

[6] Anderson, J. D., & Wendt, J. F. (1995). Computational fluid dynamics (Vol. 206). New York: McGraw-Hill.

[7] Piomelli, U. (1999). Large-eddy simulation: achievements and challenges. Progress in Aerospace Sciences, 35(4), 335-362.

[8] Hamed, A., Das, K., & Basu, D. (2004). Numerical simulations of fluidic control for transonic cavity flows. AIAA Paper, 429, 2004.

[9] Li, W., Nonomura, T., Oyama, A., & Fujii, K. (2010). LES Study of Feedback-loop Mechanism of Supersonic Open Cavity Flows. AIAA paper, 5112, 2010.

[10] Vijayakrishnan, K. (2014) Unsteady RANS computations of supersonic flow over two dimensional cavity using OpenFOAM-A validation study. AIAA 2014.

[11] Sousa, R. G., et al. (2016). Lid-driven cavity flow of viscoelastic liquids**.** Journal of Non-Newtonian Fluid Mechanics, 234, 129-138, 2016.

[12] Tuerke, F., Pastur, L. R., Sciamarella, D., Lusseyran, F., & Artana, G. (2017). Experimental study of double-cavity flow. Experiments in Fluids, 76, 2017.